

Tethered Tool Manipulation Planning with Cable Maneuvering

Daniel Sánchez¹, Weiwei Wan^{1,2*} and Kensuke Harada^{1,2}

Abstract—In this paper, we present a planner for manipulating tethered tools using dual-armed robots. The planner generates robot motion sequences to maneuver a tool and its cable while avoiding robot-cable entanglements. Firstly, the planner generates an Object Manipulation Motion Sequence (OMMS) to handle the tool and place it in desired poses. Secondly, the planner examines the tool movement associated with the OMMS and computes candidate positions for a cable slider, to maneuver the tool cable and avoid collisions. Finally, the planner determines the optimal slider positions to avoid entanglements and generates a Cable Manipulation Motion Sequence (CMMS) to place the slider in these positions. The robot executes both the OMMS and CMMS to handle the tool and its cable to avoid entanglements and excess cable bending. Simulations and real-world experiments help validate the proposed method.

I. INTRODUCTION

THE introduction of robots to manufacturing industries aims to reduce human workload, increase productivity, and decrease operation costs. Towards realizing these goals, robots must be able to adapt to industrial environments, work alongside humans, and manipulate tools to complete given tasks. Particularly, motion planning for handling tools represents a unique challenge for planners: The tool acts as a dynamic obstacle when it is being manipulated by the robot and its position and orientation during the manipulation task must be accurately computed to avoid robot-object and object-environment collisions. The tool manipulation problem gets considerably more complicated when the tool is tethered (possesses a cable). Cables are soft and dynamic obstacles for motion planning – Their position and orientation are considerably hard to compute due to their nature. The cable shape changes according to the robot actions, the tension applied to it, and the cable elasticity. These properties cause uncertainty and complicate the avoidance of robot-cable and obstacle-cable collisions. Furthermore, when the robot end-effector rotates around the tool cable, it can get snarled around the robot hand, producing undesired entanglements and cause damage to the robot and the tool. Thus, preventing robot-cable entanglements is an important goal for tethered tool manipulation.

In this paper, we present a planner for manipulating tethered tools using dual-armed robots. The planner is motivated by human manipulation strategies widely seen in our daily life. Fig.1 shows an example. The human in the figure handles a tethered tool using both arms: One arm is used for manipulating the tool; The other is used for manipulating the cables. Following this strategy, we develop a dual-arm tethered tool manipulation planner which generates an Object Manipulation

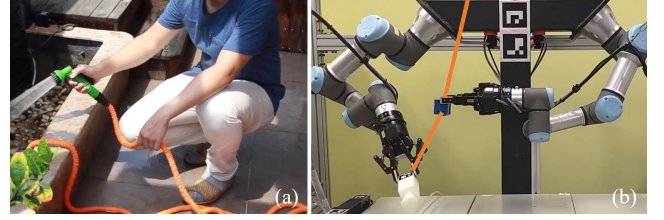


Fig. 1: (a) A human handles a tethered tool using both arms: One arm is used for manipulating the tool; The other is used for manipulating the cables. (b) The proposed planner motivated by the human strategy.

Motion Sequence (OMMS) to handle the tool, and a Cable Manipulation Motion Sequence (CMMS) constrain the cable. The planner can prevent entanglement and guarantee that the robot (1) avoids bending the tool cable in excess, and (2) avoids cable-robot and cable-environment collisions when possible.

Especially, our implementation uses a tool balancer and a cable slider. The balancer simplifies the cable deformation problem by constantly applying a pulling force, which forces the cable to form a straight line, facilitating the obstacle-avoidance computations. The cable slider is a self-designed mechanical device attached to the tool cable. The slider stuck to the cable when it is not held by the robot. When it is pressed the slider is released, and it allows the cable to slither through a central hole freely. Fig.1(b) shows the robot, its working environment as well as the cable slider (the blue box held by the right arm). The tool balancer is not shown, but it is hanged overhead straightening the cable. Besides the developed planner, this paper also provides a metric to evaluate the cable state or snarling around the robot end-effector, which can be used to compare our solution to other methods. The planner guarantees minimal robot-cable contact and avoids undesired entanglements by preventing excess bending. Simulations and real-world experiments help validate the presented solution.

II. RELATED WORK AND CONTRIBUTION

This paper develops a motion planning solution for tethered tool manipulation using dual-armed robots. It emphasizes the prevention of entanglements to increase robot safety and manipulation success rates. Accordingly, this section reviews related publications on motion planning and manipulation planning, with particular attention given to cable-like objects.

A. Motion planning

A considerable amount of publications are aimed to develop robot motion planning [1]. Early and influential work on

¹Graduate School of Engineering Science, Osaka University, Japan.

²National Inst. of AIST, Japan.

Contact: Weiwei Wan, wan@hlab.sys.es.osaka-u.ac.jp

motion planning include algorithms for path planning [2] as well as approaches based on fuzzy logic [3], [4], genetic algorithms [5], [6], and neural networks [7], [8].

Nowadays, more refined methods for motion planning have been proposed. For example, in [9] a model predictive control algorithm based on probabilistic inference through a learned predictive image model is presented. The algorithm is used to plan for actions that move user-specified objects in the environment to user-defined locations. [10] presents a methodology for nonuniform sampling to accelerate sampling-based motion planning. In [11], a discrete RRT algorithm for path planning is shown. [12] shows an integrated motion planning and scheduling method for human and industrial-robot collaboration.

B. Manipulation planning

Manipulation planning can be considered as a constrained case of motion planning. The motion sequences generated by manipulation planning allow the robot to move objects and to modify its environment's structure [13]. The planning process takes into account the movement of the robot in an environment with movable (manipulated) objects in addition to the environment static obstacles.

Recently, manipulation planning has been the focus of several work such as algorithms for single-arm and dual-arm object pick-and-place using regrasps [14], a probabilistically complete planner for prehensile and non-prehensile actions in cluttered environments [15], an algorithm to preserve object stability under changing external forces [16], planning solutions for manipulating an elastic object from an initial to a final configuration [17], a planning framework that uses non-prehensile actions for the rearrangement of clutter and manipulation of object pose uncertainty [18], and a manipulation planner for the cleaning of planar surfaces [19].

C. The manipulation planning of cable-like objects

In particular, motion planning and manipulation planning for handling cables or cable-like objects represents a challenging task. Several strategies have been proposed to solve the task. For example, a study on quasi-static manipulation of a planar kinematic chain is presented in [20]. A control solution, for the manipulation of a fire hose, was shown in [21]. A planner for manipulation of interlinked deformable linear objects for aircraft assembly was shown in [22]. A planning method for knotting/unknotting of deformable linear objects [23], and a motion planner to manipulate deformable linear objects is described in [24].

D. Contributions

The work mentioned above presents solutions for manipulating cable-like objects, but they do not address robot-cable entanglement avoidance or excessive bending. The definition of cable entanglement can be subjective. In theory, if the robot avoids collision with the tool cable, there will be no entanglements. However, in practice, contact between the robot arm and the cable is often unavoidable. In such cases, it

is important to establish a criterion to differentiate between dangerous cable collisions and unavoidable but manageable robot-cable contact. We do so by defining the angle accumulation concept and design a planner that tries to diminish the accumulated angle.

In one of our previous work [25], we presented a planning solution for regrasp manipulation of tethered tools with tool balancers, but that solution was based on avoiding robot poses or motions that could cause entanglements. The solution helped to avoid collisions with the cable but significantly diminished the freedom of movement of the robot. Unlike the previous solution, in this work, we generate a motion sequence to manipulate both the cable and the tool and diminish cable collisions. The cable maneuvering motions are performed to control the cable bending angle and keep it away from others.

III. MANIPULATION PLANNING FOR TETHERED TOOLS

The present method for tool manipulation employs a tool balancer to suspend the manipulated tools. A tool balancer is a device that provides a cable to hang tools. The cable presents a constant pulling force that simplifies the cable deformation problem by making the cable form a straight line between its endpoint and the tools connection point, as seen in Fig.2.

In our case, the installation of the tool balancer plays a key role in the success of tool manipulation. The initial position of the tool balancer was chosen using a manipulability-reachability based rating method. The method is used to determine the best starting positions for the balancer.

The planner computes two motion sequences to realize tethered tool manipulation. The first motion sequence is an Object Manipulation Motion Sequence (OMMS), which is computed using our previously proposed single-arm manipulation planner [14] to manipulate the tool and place it in the desired pose. The second sequence, the Cable Manipulation Motion Sequence (CMMS), is used to modify the tool cable shape: The robot manipulates a cable slider to control the bending and the position of the cable. The CMMS diminishes the occurrence of robot-cable collisions by placing the cable directly behind the tool during its manipulation.

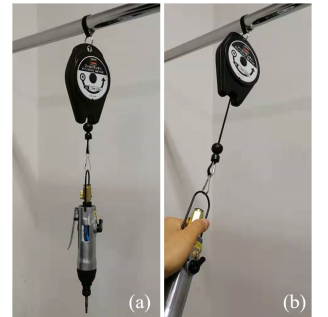


Fig. 2: The cable of the tool balancer presents a constant pulling force that simplifies the cable deformation into a straight line.

A. Cable angle accumulation and entanglement avoidance

In principle, if the robot avoids any contact between the cable and itself or the environment, then it can avoid entanglements entirely. In practice though, these conditions are not always possible since the robot end-effector is usually close to the tool cable. Furthermore, slight contact between the end-effector and the tool cable can be tolerated if it does not represent a risk for either.

To tackle this problem, we introduce the concept of angle accumulation. Angle accumulation represents the extra rotation of the cable around a collision point in the end-effector – If the tool cable collides with the robot end-effector, subsequent rotations around the collision point will cause the cable to get more snarled around the robot. Thus, it is important to prevent or diminish angle accumulation. Fig.3 helps illustrate the concept. The figure shows a 2D simplification the angle accumulation problem. By representing the tool cable as a straight line (thanks to the tool balancer) and measuring the angle of bending at the tool reference frame, we can determine if the cable stays within a permissible zone. If the tool cable bending (measured as 0 when the cable is in the α_r reference state, equivalent to the α_0 state in Fig. 3), stays within the permissible states (its bending angle does not surpass the angle of grasping β or 90 degrees), we can assume the cable will not collide with the end-effector or the tool itself. If on the other hand, the cable bending goes beyond the maximum angle β , we say it is in a state of angle accumulation around the end-effector. If the cable surpasses the 90 degrees of bending while rotating clockwise (using Fig.3 as reference) we say the cable is in a state of angle accumulation around the tool. To calculate the angle accumulation around the end-effector for a cable state α_i , we use Eq.(1) to compute the accumulation magnitude:

$$A_{cc}(i) = \begin{cases} 0 & \text{if } \angle \alpha_r T \alpha_i < \beta, \text{ else} \\ A_{cc}(i-1) + \eta_\theta(\alpha_i) \{ \angle \alpha_r T \alpha_i - \angle \alpha_r T \alpha_{i-1} \} - \beta & \end{cases} \quad (1)$$

Here, α_r represents the cable with no bending, equivalent to α_0 in Fig.3. T is the connection point between the cable and the tool. α_i is the i -th cable state, which is represented as a vector or a straight line that goes from the tool tail to the cable anchor point (tool balancer or cable slider). Basically, the function adds up the differential changes in angle between cable states α_i and the reference state α_r . The value of $\eta_\theta(\alpha_i)$ acts as a memory variable with values that depend on the cable position, based on the quadrants at the tool local reference frame, the value of $\eta_\theta(\alpha_i)$ is described by Eq.(2):

$$\eta_\theta(\alpha_i) = \begin{cases} 1 & \text{if } \alpha_i \in \text{quadrants 1 or 2} \\ -1 & \text{if } \alpha_i \in \text{quadrants 3 or 4} \end{cases} \quad (2)$$

The variable $\eta_\theta(\alpha_i)$ is used to correct the addition of differential accumulation when the cable enters quadrants 3 and 4 shown in Fig.3. For example, If the cable starts at state α_0 and rotates counter-clock wise, we must adjust the sign of the magnitude $\angle \alpha_0 T \alpha_i - \angle \alpha_0 T \alpha_{i-1}$ after the cable surpasses state α_4 , otherwise, the differential sum $\angle \alpha_0 T \alpha_i - \angle \alpha_0 T \alpha_{i-1}$

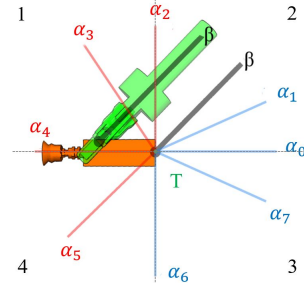


Fig. 3: A 2D illustration of angle accumulation. If the cable bending angle (blue and red segments) surpasses the angle of grasping or 90 degrees, the cable starts to get snarled around the end-effector (red segments). The arabic numbers indicate the quadrants in the tool reference frame.

will be negative and the angular accumulation will decrease when, in reality, the cable is getting more snarled around the end-effector.

To calculate the angle accumulation around the tool, (for clock-wise rotations, using Fig.3 as reference) we can use:

$$A_{cc}(i) = \begin{cases} 0 & \text{if } \angle \alpha_r T \alpha_i < 90, \text{ else} \\ A_{cc}(i-1) + \eta_\theta(\alpha_i) \{ \angle \alpha_r T \alpha_i - \angle \alpha_r T \alpha_{i-1} \} - 90 & \end{cases} \quad (3)$$

where $\eta_\theta = -\eta_\phi$. To determine if the angle accumulation is around the tool or the end-effector, we can check in which quadrant the cable is located when its bending surpasses 90 degrees or β respectively.

B. High manipulability region

The initial installation position of the tool balancer is an important factor in successful manipulation planning. A non-optimal installation position can pose the tool and cable slider in difficult to grasp positions, hindering the planner ability to find a solution for a given manipulation task.

Intuitively, the effectiveness of our planner depends on the initial position of the tool balancer. If the balancer is too far from the robot, the number of IK-feasible grasps of the cable slider and the tool decreases. On the other hand, if the tool balancer is too close to the robot, the maneuvering space for the tool cable could be too small, increasing the risk of robot self-collision. Also, the robot should be able to grasp the tool and the cable using both arms, so the balancer must be centered in front of the robot.

Following these considerations, we optimize the initial installation position of the tool balancer by using a rating method based on the robots reachability and manipulability. Our rating method computes the most advantageous positions for the tool balancer and is also used to compute a region of high manipulability.

1) *Grasp-based reachability region for dual armed robots:* An optimal tool balancer position can help the planner by (1) placing the tool and its cable in a position of high reachability and manipulability, and (2) giving the robot enough room to maneuver the tool and the cable. We employ a reachability test for the robot workspace to find balancer positions that comply with both requirements, to find an optimal balancer position.

Firstly, we map the workspace into several points in a grid separated by 50 mm each. Secondly, we tasked our IK-solver to generate IK solutions to place the robot end-effectors in every point of the grid. The points with at least one IK solution are cataloged as reachable.

These reachable points are then used to map the robot workspace with regions of reachability Ω_r and Ω_l for the right and left arms respectively. A region of dual-arm reachability can be computed by intersecting Ω_r and Ω_l like in Eq.(4):

$$\Omega = \Omega_r \cap \Omega_l \quad (4)$$

The resulting region, Ω contains candidate positions for the tool placement. Since the tool balancer is used to hang the tool vertically, once the horizontal or x and y coordinates of the balancer (in the robot reference frame) are set, the tool and the cable slider can only change their resting position in the

vertical axis. We aim to find a position in the robot horizontal plane (x - y plane) that maximizes the dual-arm reachability in the robot vertical axis.

To choose the optimal x and y coordinates for the balancer position, we evaluate each x - y coordinate pair in our grid by counting the reachable points in their vertical axis. That is, we fix the x and y coordinates and test the reachability of the points in the vertical axis z , increasing the height 50 mm at a time. The x -axis in the robot reference frame points to the robot front, the y -axis points to the robot left-hand side and the z -axis points upwards.

From our analysis, the coordinate pair (300,0)[mm] (300 mm in front of the robot, centered between its arms) yielded the highest amount of evaluated reachable points along the vertical axis z , with 15 reachable points. Nonetheless the x - y coordinate pair is dangerously close to the robot frame, which significantly impairs our CMMS since the CMMS normally places the cable-holding arm behind the tool-handling arm, leading to very close motion and a small zone near the robot body. To avoid these problems, we decided to place the tool balancer farther in front of the robot, at the coordinates (450, 0, 1800)[mm] at the cost of selecting a pair of x - y coordinates with 14 reachable points along the z -axis.

2) *Grasp-based manipulability analysis*: The CMMS involves motions to make the cable-holding arm follow the movement of the tool while grasping a cable slider. Usually, these motions place the cable-holding arm in a region between the robot-body and the tool-handling arm. In this region the arm robot requires high mobility to avoid collisions and complete its task. To ensure high mobility for the cable-holding arm, we would like to place the cable slider in a region with a high expected manipulability index.

The manipulability of a robot represents its ability to position and re-orientate its end-effector given an initial joint configuration. While inspecting the infinite joint configurations of the robot arm is impractical, we can perform a grasp-based analysis to obtain an expected or average manipulability based on the cable slider position and the IK-feasible grasps for that particular position. The result is an average value of manipulability associated with a point in space.

To compute the expected manipulability of a point in space, we place the slider in this point using our simulation environment. Then, we compute the IK solutions if they exist, that allows the robot to grasp the tool using the grasps stored in our grasp database [26]. For simplicity, the slider orientation is fixed to a single value when evaluating the possible grasps. Our algorithm then evaluates the manipulability of each IK solution and computes the median value for a single point in the robot workspace using Eq.(5):

$$M(p(x, y, z)) = \frac{\sum_{n=0}^{G(p(x, y, z))} m(g_n(p(x, y, z)))}{G(p(x, y, z))} \quad (5)$$

Here, M is the average manipulability score for a point $p(x, y, z)$, $G(p(x, y, z))$ is the total (non-zero) amount of IK-feasible grasps for the slider in point $p(x, y, z)$, m is a function that returns the manipulability of the robot based on its joint angles and its maximum angles of rotation and g_n is the n -th

set of joint angles that place the robot end-effector in the pose necessary to execute the n -th grasp. Fig.4 shows the process of calculating the manipulability for two different slider positions.

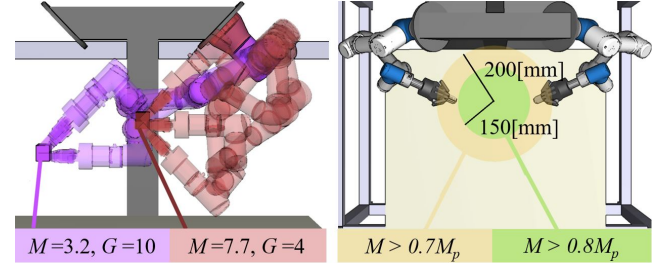


Fig. 4: Manipulability Analysis. Left: We compute the different grasps of the tool balancer for two cable slider positions. The manipulability for each grasp is calculated and added to a total value. The position with the highest average manipulability M and possible grasps G is a more desirable starting position for the slider. Right: Manipulability spheres. Within the radius of the spheres, the values M and G stay above threshold values based on a position of high manipulability and high amount of IK-feasible grasps.

Using Eq.(5), we computed the average manipulability and available grasps within the grid used in the previous sub-section. The highest average manipulability scores were registered within a certain region of the robot workspace. By using these scores, we can create a “manipulability sphere” to represent this region in which the number of possible slider grasps $G(p(x, y, z))$ and the score M stay above certain reference values. We used the coordinates (400, 0, 1450)[mm] as our reference point since it has a central location in the robot reachable zone, the coordinates yielded a M_p value for the average manipulability and G_p number of unique Ik-feasible grasps.

Afterward, we explored the remaining points in the grid and realized that, by keeping the slider within a 150 mm radius from the reference point, the manipulability and available grasps of the evaluated points stay above $0.8M_p$ and $0.5G_p$. Since the chosen tool balancer position will directly place the slider at the coordinates (450, 0, z)[mm], where the height z is variable, we can assume the initial position where the slider will most likely be within 150[mm] of the reference point and a relatively high manipulability for the initial grasp can be expected. Fig.4 shows a representation of the manipulability sphere of 150[mm] and 200[mm] and the minimum M and G values registered within these regions.

C. Object manipulation planning

The OMMS is generated in three steps using our previous planner [14]. Firstly, the planner selects a candidate object grasp C^h from a previously-built database to pick-up the object in a starting pose. The grasp database [26] is computed offline in the object’s local coordinate system Σ_t . Secondly, the planner checks the IK-feasibility and robot-object collisions of the start and goal robot grasping poses. The grasping poses are

represented by a given end-effector transformation matrix oT which can be computed using Eq.(6):

$${}^oT = C^h O^o \quad (6)$$

Here, O^o represents the transformation matrix of the tool for a given pose (starting or goal object pose) in the robots reference frame Σ_o . Finally, the planner connects the starting and goal grasping poses of the object through an intermediate/transfer robot poses generated by an RRT-based sampling method. The result is a series of motions that allow the robot to grasp an object, maneuver it through its workspace, and place it in the desired goal pose. The object movement associated with this motion sequence is subsequently used to plan the CMMS.

D. Cable manipulation planning

The CMMS is computed to control the cable-manipulating arm and place the cable in optimal positions that diminish cable angle accumulation around the end-effector and prevent robot-cable collisions. The robot handles the cable using a slider tool, as seen in Fig 5.

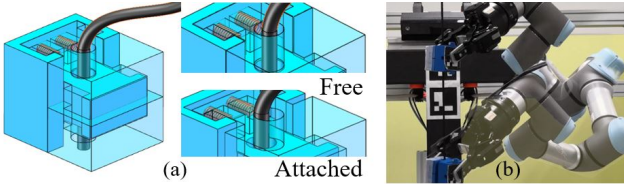


Fig. 5: (a) The cable slider model. (a-Free) The slider in its free state. When the robot gripper grasps the slider, the gripper overcomes the spring forces and pushes the two slider internal circular holes to a concentric state, allowing for the free movement of the cable through both holes. (a-Attach) The slider in its attached state. When it is not being manipulated, its internal springs apply a constant force, constraining the cable. (b) The robot manipulating the slider in its free state.

The cable can slide through the slider, simplifying the cable manipulation problem to a slider placement problem. To generate a CMMS and avoid entanglements, our planner selects one of the possible slider grasps and generates the motions necessary to reach the selected grasp. Subsequently, the planner computes the tool motions associated with the OMMS and estimates the optimal cable positions for every intermediate state of the tool generated by RRT-based exploring. The result is a motion sequence that allows the robot to reach and grasp the cable slider and control the cable movement, placing it directly behind the tool if possible, preventing collisions and excess angle accumulation between the end-effector and the cable.

The OMMS is used to calculate the poses of the tool during the manipulation process and generate the CMMS. For each tool pose, the planner computes a projection from the tool's tail (connection point between the tool and its cable). The projection will be used as goal positions for the slider

tool. Each projection position op (as described in the robots reference frame Σ_o) can be computed using Eq.(7):

$${}^op = {}^oR_t \alpha_s {}^t\mathbf{v} + {}^oq + {}^oh, \quad (7)$$

where oR_t represents the tools rotation matrix. ${}^t\mathbf{v}$ is an unitary vector in the tool's reference frame Σ_t . It points to the tool tail normal direction. The scalar value α_s dictates the magnitude of the projection or how far behind the tool the cable slider should be placed. The object's position oq is added to place the projection in the correct position in the robot's reference frame. Finally, the vector oh is added to translate the projection point vertically in order to maintain a minimum height for the slider position (to avoid collisions with the table). Fig.6 better illustrates this process. The planner then examines every point op as a candidate goal position for the cable-holding arm.

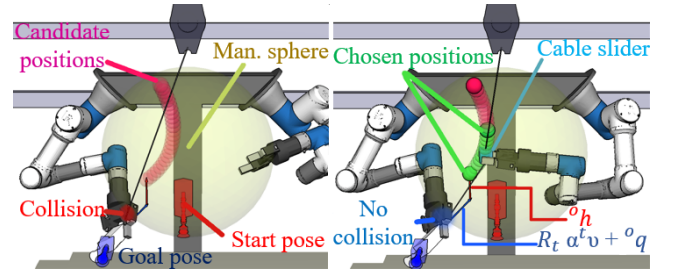


Fig. 6: Simulated OMMS-only and OMMS+CMMS tool manipulation. Left: The robot executes an OMMS with its right arm. The planner uses the vectors ${}^oR_t \alpha_s {}^t\mathbf{v} + {}^oq$ (in blue) and oh (red) to calculate candidate positions for the cable slider (represented by the purple spheres) by using the vectors. Right: The robot moves the cable slider to selected candidate positions. The chosen positions (green spheres) minimize the bending angle of the cable and prevent collisions. Abbreviation: Man. sphere – Manipulaiton sphere.

Discarding slider positions: Each slider position is linked to its corresponding object pose and the pose of the tool manipulating arm (dictated by the OMMS), to form a list P of candidate slider poses. The corresponding robot poses, object position, and slider candidate position are used to verify collision avoidance. To perform collision detection, we assume the cable shape is represented by two straight lines, the first line goes between the tool and the slider, and the second, between the slider and the balancer, both lines can be represented as vectors. With the line vectors, we can check if the robot collides with the cable during manipulation. Also, we can measure the angle between the cable (the section that goes from the tool to the slider) and the end-effector to verify if there is angle accumulation.

Ideally, the robot can place the slider in all its candidate position points without collisions. If there are points in P that are either, not reachable by the robot, cause cable collisions (disregarding the robot end-effector), or surpass the angle accumulation threshold, the planner discards them and uses RRT exploring to connect the closest adjacent points that do not violate these conditions.

In the case the planner does not find a motion sequence that preserves the angle accumulation below a given threshold (30

degrees in our case) for all the robot states, the planner can compute the goal positions again by reducing α_s by 20%. If it fails to find a solution again, the planning fails and a new OMMS must be computed again to find an alternative CMMS.

IV. EXPERIMENTS AND ANALYSIS

A. Angle accumulation measurements

Several benchmarks to test the performance of the proposed planner using our simulation environment^a are performed. For these tests, the robot right arm manipulates the object, and the left-hand maneuvers the cable, the threshold for maximum angle accumulation is set to 30°.

Each benchmark consists of an initial tool pose and three-goal poses. The planner generates motion sequences to pick up the tool and then place it in the desired goal poses. Seven different goal poses are considered to create a benchmark. The poses are shown in Fig.7. For each simulation, we track the angle accumulation of the robot right arm for later analysis. Also, we used the OMMS-only planner and a planner that uses object handover to complete the same tasks and compare the planners.

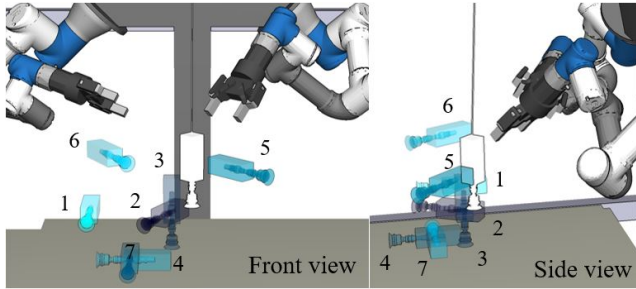


Fig. 7: Goals for the simulation benchmarks. The blue transparent objects represent the candidate goal poses of the tool. For each benchmark, the robot must grasp the object in its initial pose (white), and place it in three of the randomly chosen goal poses.

Table I shows the goals chosen for each benchmark (benchmark number in bold and in parenthesis) and the maximum and mean angle accumulation (mean in bold and parenthesis) for each solution.

The CMMS allows the robot to handle the tool cable to follow the movement of the tool, reducing cable bending at the tool local reference frame. On average, the OMMS+CMMS executions reduced maximum angle accumulation by 50% when compared to the OMMS-only planner and by 67% when compared to dual handed tool manipulation. The average angle accumulation for the OMMS+CMMS manipulation tasks was also considerably lower for the OMMS+CMMS planner, which hints at a lower chance of end-effector-cable entanglements.

^aFor more information about our planner and simulation environment, please visit: https://gitlab.com/wanweiwei07/wrs_nedo

TABLE I

Goals	A_{cc} [degrees]
(1) 1, 6, 3	O+C = 27.61 (6.06), O = 42.43 (16.88), H = 83.75 (27.14)
(2) 2, 1, 3	O+C = 16.56 (2.89), O = 44.59 (17.88), H = 44.59 (14.21)
(3) 3, 4, 5	O+C = 16.49 (2.20), O = 45.0 (22.16), H = 82.48 (19.95)
(4) 4, 1, 5	O+C = 16.70 (2.31), O = 44.96 (24.38), H = 80.65 (23.55)
(5) 7, 6, 2	O+C = 29.83 (6.02), O = 44.12 (23.64), H = 75.12 (26.95)
(6) 5, 4, 1	O+C = 25.05 (4.48), O = 43.89 (27.25), H = 44.99 (18.74)

Meanings of abbreviation: O+C represents the OMMS+CMMS solution for the given benchmark. O is the OMMS-only solution. H represents the solutions using handover.

B. OMMS+CMMS without the tool balancer

A downside of the tool balancer is that it does not allow for the regrasping of the tool using table placements (the cable would pull the tool out of position). If regrasping is necessary, the robot is forced to use handover motions, the motions with the highest angle accumulation. The proposed planner can also be used to maneuver tethered tools without the use of a tool balancer, allowing the tool handling arm to perform regrasps using table placements.

In this case, one end of the cable is fixed to a corner of the robot table to approximate the cable shape as two straight lines, which go between the tool and the cable slider and between the cable slider and the fixed point.

By manipulating the tool cable the robot can not only diminish angle accumulation and the possibility of entanglements, as shown in the previous experiment, but it can also maneuver the cable above obstacles in the robot workspace.

Obstacle-avoidance experiments are performed to test the balancer-less planner. The experiments consist of randomly placing a box as an obstacle in the robot workspace and performing a manipulation task with a tool starting pose, and two-goal poses. The planner is tasked to place the tool in two-goal positions, and the amount of cable-obstacle collisions are measured for each planner. Ten different tests are performed with random box positions using our planner and the OMMS-only planner. The straight-line cable approximation is used to detect collisions in our simulation environment. Real tests are performed to assess collisions with the obstacles.

C. Real-world experiments

After testing our planner in simulations, we applied our solution to our real-world robot. The robot uses its hand-mounted cameras to detect the AR Markers on the tool and the slider and compute their current pose. For these experiments, we tested the same motion sequences planned in our simulations.

In all cases, the robot was able to complete the OMMS+CMMS task while manipulating the cable. In Fig.8 a real-world execution of the planner performing benchmark 1 can be seen and compared to the regular OMMS-only planner and the solution provided by the planner using handover. The

angle accumulation comparison between planners for benchmarks 1 through 6 is shown in Fig.9. A video demonstration can be seen in the supplementary material.

Furthermore, we also executed the cable-box collision avoidance motion sequences. An example can also be seen in Fig.8. Table II shows the results of real-world executions. The presented planner avoids collisions in 70% of the cases while the OMMS-only planner is only successful in 20% of the cases. The cable shape is assumed to be a straight line for the OMMS + CMMS planner since the robot holds the cable slider close to the tool. The same approximation cannot be used for the balancer-less, OMMS-only solution since the cable does not form a straight line, making its shape difficult to predict. A video demonstration can be seen in the supplementary material.

TABLE II

Planner	Success	Collisions	Mean A_{cc} [degrees]
OMMS	2	8	N/A
OMMS + CMMS	7	3	6.81

V. CONCLUSIONS

In this paper, we presented a manipulation planner for entanglement avoidance. Simulations and real-world experiments confirm that the planner generates motion sequences that reduce angle accumulation around the robot end-effector and allow collision avoidance between the cable and the robot and the cable and its environment. The tool balancer provides a constant pulling force for the cable, straightening its shape and simplifying collision detection and the computation of the cable shape. On the other hand, the balancer limits the regrasping capabilities of the robot. Furthermore, the experiments without the tool balancer showed that the CMMS allows the robot to manipulate the cable to avoid obstacles and also perform tool regrasping by using placements. Cable obstacle avoidance can be especially useful in cluttered environments where the cable could push objects outside of the robot reach or disturb the original positions of obstacles and objects, which can be fatal for offline manipulation planners like ours. Nonetheless, a more accurate representation of the cable catenary shape could allow a higher success rate with an increased amount of obstacles.

Our planner provides a safe alternative to tethered tool manipulation. It reduces cable bending at the tool local reference frame and angle accumulation during the manipulation task. The use of a tool balancer facilitates and makes more accurate the simulations during the planning stage, but the planner can still be implemented without the balancer to perform tool placements and regrasping. Future implementations of the proposed planner will aim to solve the cable deformation problem and discard the need for a tool balancer.

REFERENCES

- [1] E. Masehian and D. Sedighizadeh, "Classic and heuristic approaches in robot motion planning-a chronological review," *World Academy of Science, Engineering and Technology*, vol. 23, no. 5, pp. 101–106, 2007.
- [2] T. Lozano-Pérez and M. A. Wesley, "An algorithm for planning collision-free paths among polyhedral obstacles," *Communications of the ACM*, vol. 22, no. 10, pp. 560–570, 1979.
- [3] G. Vachtsevanos and H. Hexmoor, "A fuzzy logic approach to robotic path planning with obstacle avoidance," in *IEEE Conference on Decision and Control*, 1986, pp. 1262–1264.
- [4] K. Walker and A. C. Esterline, "Fuzzy motion planning using the takagi-sugeno method," in *Proceedings of the IEEE SoutheastCon*, 2000, pp. 56–59.
- [5] J. K. Parker, A. R. Khoogar, and D. E. Goldberg, "Inverse kinematics of redundant robots using genetic algorithms," in *IEEE International Conference on Robotics and Automation*, 1989.
- [6] M. Gen, R. Cheng, and D. Wang, "Genetic algorithms for solving shortest path problems," in *IEEE International Conference on Evolutionary Computation*, 1997.
- [7] M. Zacksenhouse, R. J. DeFigueiredo, and D. H. Johnson, "A neural network architecture for cue-based motion planning," in *IEEE Conference on Decision and Control*, 1988, pp. 324–327.
- [8] C. Kozakiewicz and M. Ejiri, "Neural network approach to path planning for two dimensional robot motion," in *IEEE/RSJ International Workshop on Intelligent Robots and Systems*, 1991, pp. 818–823.
- [9] C. Finn and S. Levine, "Deep visual foresight for planning robot motion," in *IEEE International Conference on Robotics and Automation (ICRA)*, IEEE, 2017, pp. 2786–2793.
- [10] B. Ichter, J. Harrison, and M. Pavone, "Learning sampling distributions for robot motion planning," in *IEEE International Conference on Robotics and Automation (ICRA)*, 2018, pp. 7087–7094.
- [11] K. Solovey, O. Salzman, and D. Halperin, "Finding a needle in an exponential haystack: Discrete rrt for exploration of implicit roadmaps in multi-robot motion planning," *The International Journal of Robotics Research*, vol. 35, no. 5, pp. 501–513, 2016.
- [12] S. Pellegrinelli, A. Orlandini, N. Pedrocchi, A. Umbrico, and T. Tollo, "Motion planning and scheduling for human and industrial-robot collaboration," *CIRP Annals*, vol. 66, no. 1, pp. 1–4, 2017.
- [13] R. Alami, J.-P. Laumond, and T. Siméon, "Two manipulation planning algorithms," in *Proceedings of WAFR*, 1994, pp. 109–125.
- [14] W. Wan and K. Harada, "Developing and comparing single-arm and dual-arm regrasp," *IEEE Robotics and Automation Letters*, vol. 1, no. 1, pp. 243–250, 2016.
- [15] C. R. Garrett, T. Lozano-Pérez, and L. P. Kaelbling, "Backward-forward search for manipulation planning," in *IEEE/RSJ International Conference on Intelligent Robots and Systems (IROS)*, 2015.
- [16] L. Chen, L. F. Figueredo, and M. Dogar, "Manipulation planning under changing external forces," in *IEEE/RSJ International Conference on Intelligent Robots and Systems*, 2018, pp. 3503–3510.
- [17] F. Lamiriaux and L. E. Kavraki, "Planning paths for elastic objects under manipulation constraints," *The International Journal of Robotics Research*, vol. 20, no. 3, pp. 188–208, 2001.
- [18] M. R. Dogar and S. S. Srinivasa, "A planning framework for non-prehensile manipulation under clutter and uncertainty," *Autonomous Robots*, vol. 33, no. 3, pp. 217–236, 2012.
- [19] D. Martínez, G. Alenya, and C. Torras, "Planning robot manipulation to clean planar surfaces," *Engineering Applications of Artificial Intelligence*, vol. 39, pp. 23–32, 2015.
- [20] Z. McCarthy and T. Bretl, "Mechanics and manipulation of planar elastic kinematic chains," in *IEEE International Conference on Robotics and Automation*, 2012, pp. 2798–2805.
- [21] I. G. Ramirez-Alpizar, M. Naveau, C. Benazeth, O. Stasse, J.-P. Laumond, K. Harada, and E. Yoshida, "Motion generation for pulling a fire hose by a humanoid robot," in *IEEE-RAS International Conference on Humanoid Robots*, 2016, pp. 1016–1021.
- [22] A. Shah, L. Blumberg, and J. Shah, "Planning for manipulation of interlinked deformable linear objects with applications to aircraft assembly," *IEEE Transactions on Automation Science and Engineering*, vol. 15, no. 4, pp. 1823–1838, 2018.
- [23] H. Wakamatsu, E. Arai, and S. Hirai, "Knotting/un knotting manipulation of deformable linear objects," *The International Journal of Robotics Research*, vol. 25, no. 4, pp. 371–395, 2006.
- [24] M. Saha, P. Isto, and J.-C. Latombe, "Motion planning for robotic manipulation of deformable linear objects," in *Experimental Robotics*, 2008, pp. 23–32.
- [25] D. Sánchez, W. Wan, and K. Harada, "Arm manipulation planning of tethered tools with the help of a tool balancer," in *IFTToMM World Congress on Mechanism and Machine Science*, 2019, pp. 2567–2576.
- [26] W. Wan and K. Harada, "Regrasp Planning using 10,000 Grasps," *IEEE/RSJ International Conference on Intelligent Robots and Systems*, 2017.

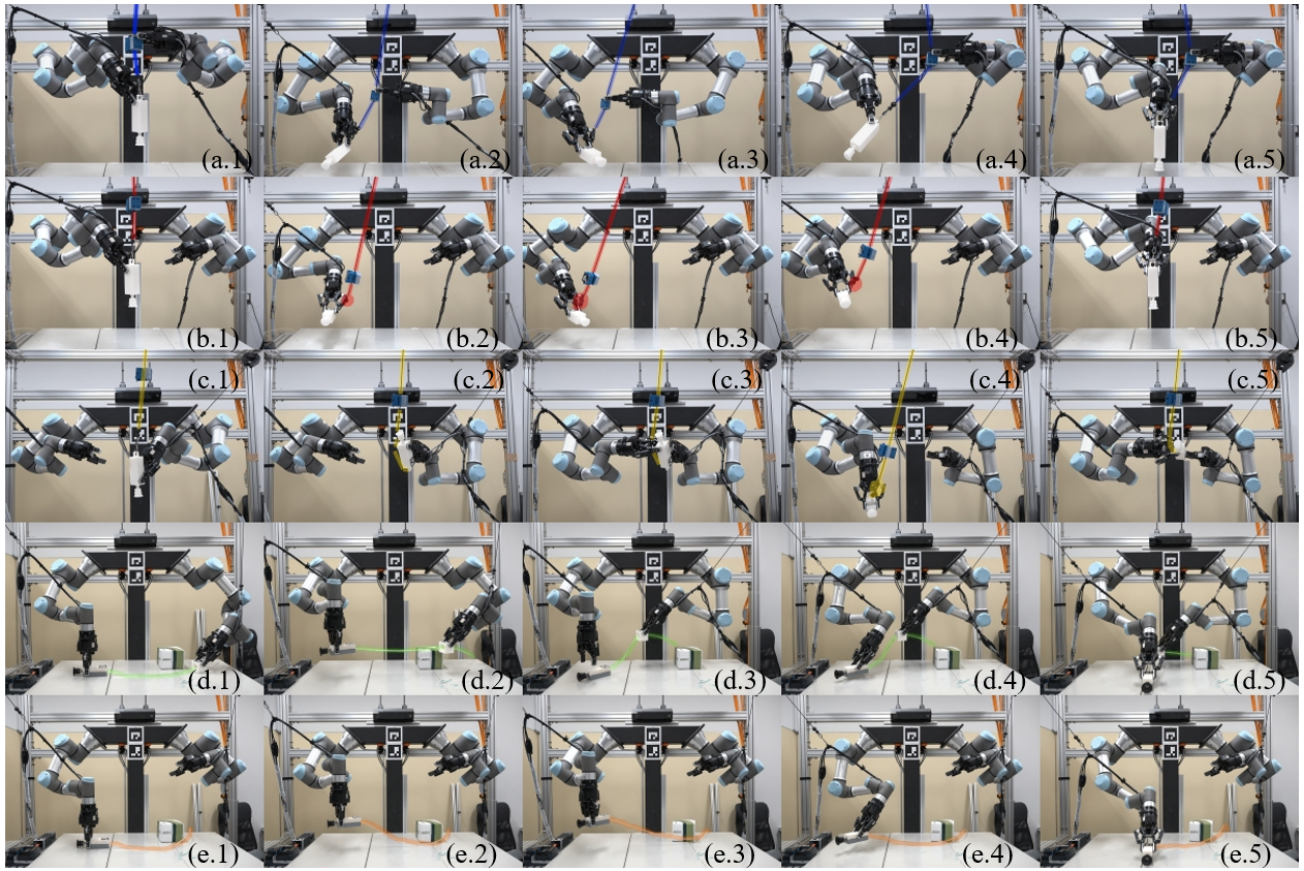


Fig. 8: Real-world implementations. The first row shows the OMMS+CMMS motion sequences – The robot completes its task without surpassing the maximum angle accumulation threshold of 30° . The second row shows the OMMS-only sequence, from the second to the fourth image we can observe the excess bending on the cable. The third row shows a part of the planner solution involving handover. In this case, the cable gets snarled around the robot end-effector when the robot performs the handover motion. Rows four and five show the OMMS+CMMS and OMMS-only solutions respectively. In the OMMS+CMMS solution, the robot successfully maneuvers the cable and avoids the obstacle by lifting it above the box. The OMMS-only solution, on the other hand, does not consider the box or the cable and results in a cable-box collision.

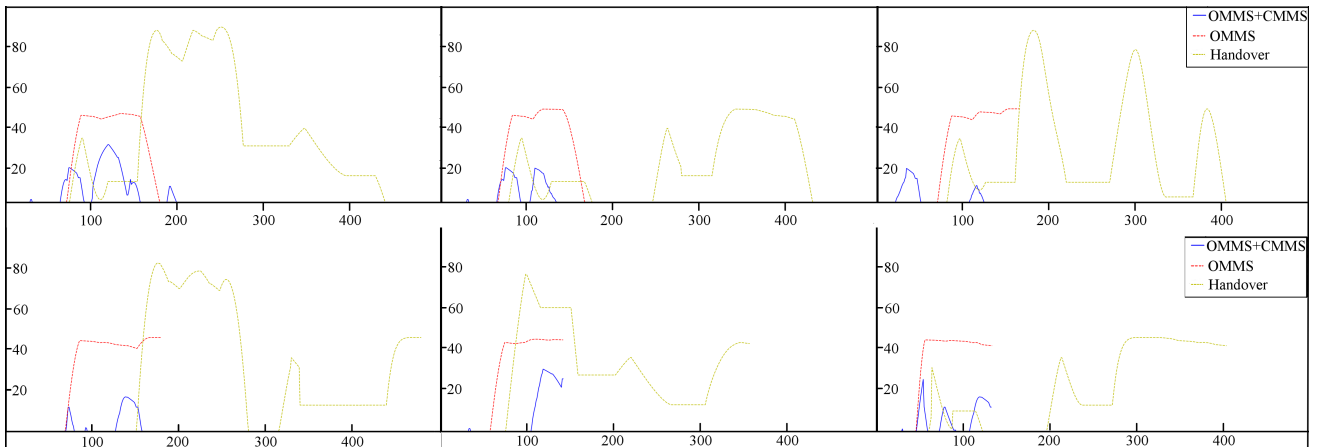


Fig. 9: Angle accumulation for the benchmarks, from the top left to bottom right graphs the figure shows the accumulation angles registered for benchmarks 1 through 6 respectively. The vertical axis shows the angle accumulation in degrees. The horizontal axis indicates the robot n-th robot state during the execution. The blue lines show the results for our OMMS+CMMS planner, the red lines show the angle accumulation for the OMMS-only planner and the yellow lines show the accumulation for the solutions with object handover.